



Current Challenges and Opportunities Toward Understanding Hydrogen Embrittlement Mechanisms in Advanced High-Strength Steels: A Review

Binhan Sun¹ · Dong Wang² · Xu Lu² · Di Wan² · Dirk Ponge¹ · Xiancheng Zhang³

Received: 24 December 2020 / Revised: 21 February 2021 / Accepted: 3 March 2021 / Published online: 13 April 2021
© The Chinese Society for Metals (CSM) and Springer-Verlag GmbH Germany, part of Springer Nature 2021

Abstract

Hydrogen embrittlement (HE) is one of the most dangerous yet most elusive embrittlement problems in metallic materials. Advanced high-strength steels (AHSS) are particularly prone to HE, as evidenced by the serious degradation of their load-bearing capacity with the presence of typically only a few parts-per-million H. This strongly impedes their further development and application and could set an abrupt halt for the weight reduction strategies pursued globally in the automotive industry. It is thus important to understand the HE mechanisms in this material class, in order to develop effective H-resistant strategies. Here, we review the related research in this field, with the purpose to highlight the recent progress, and more importantly, the current challenges toward understanding the fundamental HE mechanisms in modern AHSS. The review starts with a brief introduction of current HE models, followed by an overview of the state-of-the-art micromechanical testing techniques dedicated for HE study. Finally, the reported HE phenomena in different types of AHSS are critically reviewed. Focuses are particularly placed on two representative multiphase steels, i.e., ferrite–martensite dual-phase steels and ferrite–austenite medium-Mn steels, with the aim to highlight the multiple dimensions of complexity of HE mechanisms in complex AHSS. Based on this, open scientific questions and the critical challenges in this field are discussed to guide future research efforts.

Keywords Hydrogen embrittlement · Advanced high-strength steels (AHSS) · Damage mechanisms · Multiphase steels

1 Introduction

Hydrogen embrittlement (HE) corresponds to the abrupt loss of a material's load-bearing capacity or damage resistance in presence of H. This phenomenon was firstly documented by Johnson in 1875 [1] and has been observed in many metallic

materials including iron and steels, Ti alloys, Al alloys and superalloys [2–9]. Since the H ingress into a material is normally difficult to avoid due to the ubiquitous nature of H atoms, HE is a particularly dangerous embrittling phenomenon and often responsible for catastrophic and unpredictable failure of large-scale engineering structures [5, 10]. The concern to HE has thus triggered a considerable amount of studies in the past more than 100 years.

Among all the alloy classes, advanced high-strength steels (AHSS) are particularly prone to HE [5, 11–13]. These steels are continuously sought after in the automotive industry, in order to meet the body-in-white weight reduction strategies for fuel economy and vehicle safety. However, the ingress of typically only a few parts-per-million H can result in a serious degradation of strength and/or ductility in certain AHSS grades [11, 14]. H uptake in these materials can occur in various stages of manufacturing (steelmaking processes and car body manufacturing) as well as in service. In the former case, the embrittlement is often induced by internal H, which manifests itself by the delayed fracture phenomenon

Available online at <http://link.springer.com/journal/40195>.

✉ Binhan Sun
b.sun@mpie.de

- ¹ Max-Planck-Institut für Eisenforschung GmbH, Max-Planck-Straße 1, 40237 Düsseldorf, Germany
- ² Department of Mechanical and Industrial Engineering, Norwegian University of Science and Technology, Richard Birkelands vei 2B, 7491 Trondheim, Norway
- ³ Key Laboratory of Pressure Systems and Safety, Ministry of Education, School of Mechanical and Power Engineering, East China University of Science and Technology, Shanghai 200237, China

typically after sheet forming. In the service life of a vehicle, H normally enters into the steel when the protective layer is damaged and exposed to a wet/corrosive atmosphere. In this scenario, the failure caused by H is also referred to as external HE.

Despite extensive investigations over the last 100 years, HE is still an unsolved issue. In particular, its fundamental embrittling mechanisms have not been understood even in single-phase model alloys [8, 15–17]. A variety of embrittlement models caused by atomic H have been proposed, including hydrogen-enhanced decohesion (HEDE) [17], hydrogen-enhanced localized plasticity (HELP) [8], HEDE and HELP synergistic effect [18], hydrogen-enhanced strain-induced vacancies (HESIV) [19], adsorption-induced dislocation emission (AIDE) [20] and defactant concept [21]. Strong disagreement and polarized opinions generally exist among these models and their interplay. On the other hand, modern AHSS often possess a complex microstructure consisting of multiple phases and deformation behavior involving complex defect evolution and stress/strain localization [12, 22–27]. The change of microstructure and deformation behavior could alter the prevalent HE mechanisms and significantly influence the mechanical response in the presence of H. Although it is of great importance to visualize the full picture of HE in AHSS, the task is rather challenging given the great complexity in both HE itself and in the material class. This review is thus to highlight the most critical problems/challenges for understanding HE mechanisms in AHSS, with the intention to promote future research efforts. The review starts from a brief description about relevant HE mechanisms that might occur in AHSS. Then, some state-of-the-art micromechanical testing methods dedicated to HE investigations are overviewed. At last, the HE problems and mechanisms in two representative multiphase steels, i.e., ferrite–martensite dual-phase (DP) steels and ferrite–austenite medium-Mn steels, are critically reviewed, with the aim to highlight the multiple dimensions of complexity of HE mechanisms in complex AHSS.

2 Fundamental Hydrogen Embrittlement Models

2.1 Hydrogen-Enhanced Decohesion (HEDE)

In the H-enhanced decohesion model, it is proposed that the presence of H decreases the cohesive strength of lattice planes or interface boundaries [28, 29]. The underlying mechanism, suggested by Troiano [29], is that the electron of the H atom tends to enter the unfilled 3d shell of the iron atoms, which then increases the interatomic repulsive forces, thus decreasing the cohesive strength. However, the solubility of H in many metals is probably too low (e.g., 0.7 at ppm

inside ferritic stainless steels at 1 atm gaseous H atmosphere and room temperature [30]) to result in a significant decohesion effect, if H atoms are homogeneously distributed in the microstructure. Therefore, an important assumption for this model is that a sufficiently high H concentration needs to be accumulated at the sharp crack tip region caused by the hydrostatic stress field, which continuously weakens the interatomic bonds ahead of the crack tip [28, 31, 32]. The existence of very high concentrations of H near a crack tip has indeed been experimentally measured or modeled by some researchers [33–35]. The simulation results from Gerberich et al. [31] showed that in pure iron, the elastic stress can reach up to 20,000 MPa (near the theoretical stress of the material) at 23 nm in front of the crack tip, due to a dislocation shielding effect. Such a high stress level should be sufficient to attract H to render the decohesion effect [31]. This assumption is also consistent with the fact that the degree of HE is normally strain rate dependent and the existence of a slow propagation stage of H-induced cracks before catastrophic failure [29]. The frequently reported embrittling sites due to the HEDE mechanism are grain boundaries or interphase boundaries [13, 17], leading to an intergranular typed fracture surface. However, it has been questioned that whether H alone can cause interface decohesion, as other harmful elements such as Mn, S, P and Si can also segregate at these locations [36, 37]. Therefore, a combined effect of H and these embrittling elements on intergranular fracture has been proposed by some researchers [17]. Nevertheless, although a direct experimental evidence for the decreasing effect of H on cohesive energy is difficult to acquire, this point has been supported by numerous simulation works [38, 39]. For example, Jiang et al. [38] have calculated the ideal fracture energy (twice the surface energy) of (111) plane in Al and (110) plane in Fe using density functional theory (DFT) and found an almost linearly decreasing trend of the fracture energy as a function of H coverage. Similar behavior has also been found in the work of Alvaro et al. [4] for coincident lattice sites (CLS) $\Sigma 3$ and $\Sigma 5$ grain boundaries. Tahir et al. [40] have shown that even when the grain boundary is segregated by the cohesion-enhancing element C, the presence of H still decreases interface cohesion due to the detrimental mechanical contribution of H and a H-induced decrease in the beneficial chemical contribution of C atoms. Yamaguchi et al. [32] have further demonstrated using first-principles calculations that the reduction in the grain boundary cohesive energy is more influenced by the mobile H segregated to the newly formed crack surface.

2.2 Hydrogen-Enhanced Local Plasticity (HELP)

The H-enhanced local plasticity mechanism was firstly suggested by Beachem [41] in 1971, based on the fracture surface analysis as a function of stress intensity factor in

quenched and tempered steels and a comparison of the flow stresses in atmospheres with and without H. This model was then further developed by Birnbaum, Robertson and other researchers [9, 42, 43] based on elasticity theory and a series of *in situ* transmission electron microscopy (TEM) observations. According to linear elasticity and finite element calculations [42, 43], H can provide a shielding effect which reduces the repulsive force acting between edge dislocations and other obstacles (e.g., other parallel edge dislocations with Burgers vectors of the same sign, precipitates and interfaces). Such reduction is associated with the volumetric strain induced by H entering the lattice and the H-induced change of the constitutive moduli [9, 42]. It should be noted that the H shielding effect is only manifest when the dislocations move with the H atmospheres formed around them. Atomic simulations of H–dislocation interactions have also provided some insights on the underlying mechanisms of H-enhanced dislocation mobility, especially for the behavior of screw dislocations [44, 45]. It has been calculated by DFT that the presence of H can decrease the core energy and Peierls potential for both edge and screw dislocations in iron [44]. Itakura et al. [45] also showed an increasing screw dislocation velocity in iron for certain temperature ranges based on their first-principles calculation, which was due to the reduction of kink nucleation energy. However, different opinions emerged regarding whether H indeed increases the dislocation mobility. Song and Curtin [46, 47] have conducted a series of molecular dynamics calculations and shown that the H Cottrell atmospheres do not shield the interactions between edge dislocations in iron but rather suppress their motion. This point was recently supported by Xie et al. [48] who studied H–dislocation interaction in single crystal Al using *in situ* TEM nanocompression tests. They further claimed that the observed decreased mobility of dislocation caused by H was due to the locking effect of the formation of superabundant hydrogenated vacancies [48].

Nevertheless, the calculations based on elasticity theories successfully predict an increased mobility of dislocations upon loading (thus an enhanced plasticity) and a smaller equilibrium spacing between pileup dislocations in the

presence of H, which have indeed been observed in various metals [9, 49–51]. In this regard, the concentrated H near the tips of either brittle or ductile cracks will produce a highly localized plastic zone, which makes the materials readily achieve the plasticity limit and promotes the formation of damages (Fig. 1) [9, 16]. Therefore, the failure induced by this mechanism is intrinsically a ductile fracture mode which might occur in confined zones in the absence of macroscopic deformation (i.e., macroscopically “embrittlement”). Further experimental evidence supporting this mechanism includes (a) sometimes observed lower flow stresses in the presence of H compared with H-free specimens [9, 41, 42], (b) shallower dimples in the H-charged and fractured samples compared with the case in the absence of H [13] and (c) a higher density of dislocations just underneath the scanning electron microscope (SEM)-resolved H-induced cleavage or intergranular facets [8], observed by TEM performed on focused ion beam (FIB)-prepared specimens. It is important to mention that these results on bulk materials only provide indirect insights for the HELP mechanism. A direct evidence linking the H-enhanced plasticity and damage formation is still lacking.

2.3 Adsorption-Induced Dislocation Emission (AIDE)

Sufficient evidence has shown that H atoms are easily absorbed at free surfaces and subsurface sites [52, 53]. The adsorption-induced dislocation emission (AIDE) model, proposed by Lynch et al. [20], thus highlights the effects of surface-absorbed H on promoting dislocation emission at the surface. It is essentially a model describing the interaction between surface (either internal cracks or voids or free specimen surfaces) and H atoms (either internal diffusible H or environmental H). Unlike the HELP-associated failure mechanism where the crack propagation is promoted by the enhanced dislocation mobility close to the crack tip, the AIDE model proposes that it is the enhanced dislocation emission at the crack surface which produces crack advance (Fig. 2 [16]). Theoretical calculations have shown that H should not diffuse for more than a few atomic distances

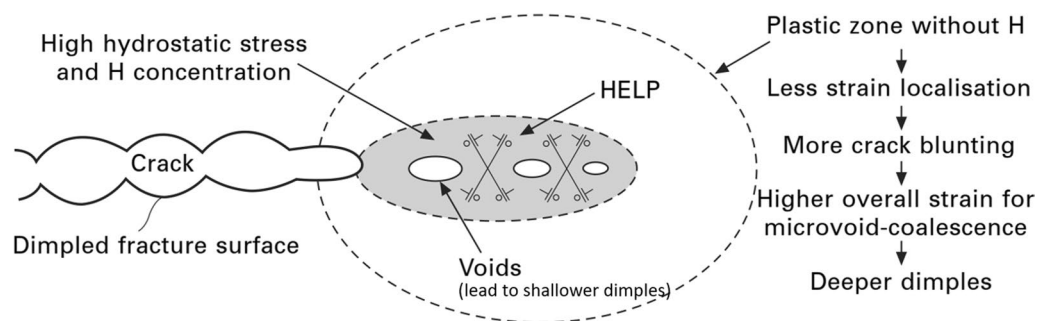


Fig. 1 Schematic diagram showing the failure mechanism induced by the HELP model. (Reprinted with permission from Ref. [20])

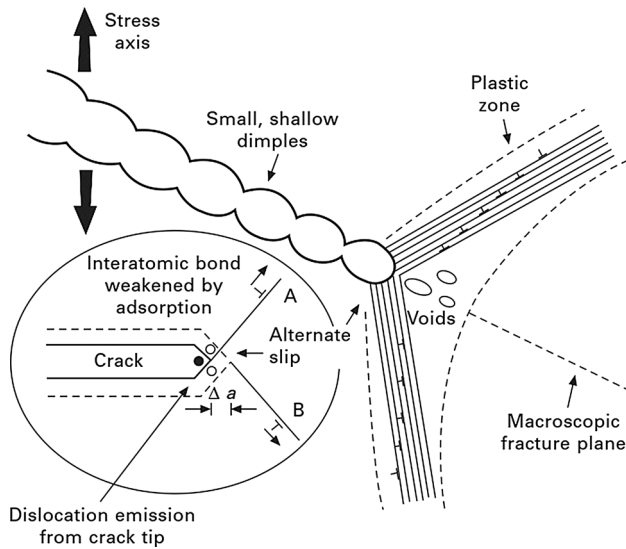


Fig. 2 Schematic diagram showing the failure mechanism induced by the AIDE model (Δa , the length of the crack growth). (Reprinted with permission from Ref. [20])

when the ratio between H diffusivity D and crack propagation velocity v , D/v , is below $\sim 10^{-8}$ cm [54]. However, HE can still occur at such “high” crack velocity. This is similar to the case of liquid–metal embrittlement (LME) where solute adsorption must occur at crack tips. Such similarity, along with other similar fractographic features between HE and LME [16, 20], provides a support for the operation of AIDE in H-induced failure.

2.4 Hydrogen-Enhanced Strain-Induced Vacancies (HESIV)

The H-enhanced strain-induced vacancies (HESIV) or H-induced superabundant vacancies model was built based on thermal desorption spectrometry (TDS) in iron and low alloyed ferritic steels [55–58]. It was observed

that a decrease in H desorption rate occurred below 200 °C at which the dislocation density was not deemed to be changed [55, 56]. Such reduction was then proposed to be the result of the annihilation of vacancies [55, 56]. Nagumo et al. [55–57] further found that the density of strain-induced vacancies deduced from the TDS data was increased with the presence of H, based on which the HESIV mechanism was proposed. This mechanism was further supported by the positron annihilation spectroscopy (PAS) where the mean positron lifetime in iron was found to be increased by tensile straining and such increase was further enhanced in the presence of pre-charged H [59]. The stabilization of vacancies due to H is also consistent with the framework of the defectants (DEFect ACTing AgeNTS) concept [60] which will be described in Sect. 2.5. The H-induced superabundant vacancies would promote the formation of vacancy clusters and very small nanosized voids, which could result in a premature fracture near the high stress/strain concentrators (e.g., crack tips). Neeraj et al. [61] have conducted careful SEM analysis on fracture surfaces in H-charged and embrittled ferritic pipeline steels. Using high surface resolution SEM parameters (3–7 kV operating voltage and 3–5 mm working distance), they found that the brittle facet that was normally observed in a lower magnification showed a “mottled” dark–bright contrast on the nanoscale (Fig. 3a, b). Such contrast was suggested to correspond to nanodimples which was supported by a careful observation of the conjugate fracture surfaces and the atomic force microscopy (AFM) results (Fig. 3c). The presence of nanodimples was then a sign of the operation of the HESIV model. However, more direct experimental evidence for this mechanism will be difficult to acquire, as both vacancies and H are extremely difficult to directly probe using current characterization techniques.

2.5 Defactants Concept

The defectants concept, introduced by Kirchheim [60] in 2009, is also a model dealing with the interaction between

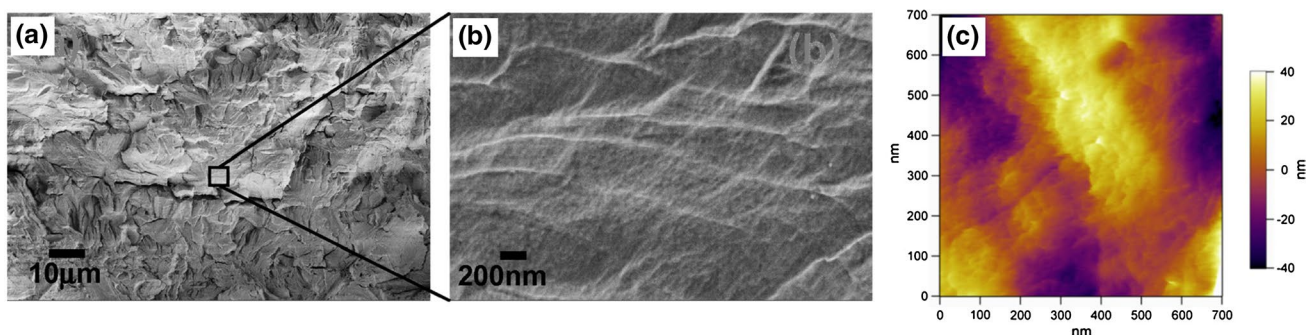


Fig. 3 **a** Fracture surface of H pre-charged and fractured X65 pipeline steel; **b** higher magnification view of the area marked in **a**; **c** atomic force microscopy (AFM) topography image from a “brittle” facet in the fracture surface of the same specimen. (Reconstructed with permission from Ref. [61])

H and defects (e.g., dislocations and vacancies). It is proposed that H, acting as a defactant, reduces the formation energy of defects in a manner analogous to the case that surfactants reduce the surface energy of liquids [21, 62, 63]. The relation between defect density ρ (e.g., grain boundary area, dislocation length and vacancies per volume V) and the amount of defactant atoms such as H has been defined as [21, 60, 62]:

$$\Gamma_H \equiv \frac{1}{V} \frac{\partial n_H}{\partial \rho} \Big|_{V, T, \mu_H, n_B}$$

where Γ is excess defactant which is positive, and n_H , n_B , T , μ are the number of H atoms, number of solvent atoms, temperature and chemical potential, respectively. This concept thus provides a thermodynamic foundation for the aforementioned HELP, AIDE and HESIV effects, i.e., accelerated generation of dislocations and vacancies due to the segregation of H atoms. It can explain both the easier nucleation of dislocations which the elasticity theory does not cover [42, 43] and the H-enhanced dislocation mobility driven by the reduction of the formation energy of kink pairs. The former phenomenon was strongly supported by recent nanoindentation tests on coarse grained materials where a clear reduction of pop-in loads was observed for the tests conducted under H compared with the H-free condition [64, 65].

3 Summary of Hydrogen Embrittlement Micromechanisms

Sections 2.1–2.5 only provide a brief description of five fundamental HE mechanisms that might occur in AHSS. More systematic and detailed review for each model can be found elsewhere [8, 17, 19–21]. Other HE mechanisms such as the high-pressure molecular H-induced failure (or internal pressure theory) [66] and hydride-induced failure are not covered here, as they only become dominant in specific circumstances, e.g., in the presence of supersaturated H [67] or hydride-forming elements (V, Zr, Nb, Ta and Ti) [68]. Among the aforementioned HE models (Sects. 2.1–2.5), only the HEDE mechanism produces a pure brittle failure, while other mechanisms result in an intrinsically ductile failure even though sometimes the SEM-resolved fracture surface might show some brittle-like facets. Although polarized opinions exist pertaining to the prevalence of different models, they generally do not repel each other and can operate synergistically for the premature fracture of materials. For example, the enhanced dislocation activity due to HELP or AIDE might promote the formation of strain-induced vacancies and activate the HESIV mechanism [20, 61]. The higher density of pileup dislocations due to the HELP effect might facilitate H transport to the obstacles

(e.g., grain boundaries), thus promoting the occurrence of the HEDE effect [18]. In view of this, it is thus highly possible that not only one HE mechanism exists especially in complex heterogeneous materials like most AHSS, which will be further discussed in Sect. 4.

4 Advanced in situ and Micromechanical Testing Techniques for Hydrogen Embrittlement Investigation

The conventional approach to detect H effect is to conduct mechanical tests on a H-charged bulk sample in comparison with an uncharged one. The analysis of the degradation of mechanical properties and fracture behavior provides useful information on the HE phenomena. However, HE is a complex process that is affected by many intrinsic compositional and microstructural features and extrinsic variables (e.g., loading atmosphere, strain rate, etc.). These large-scale tests are thus not capable to fully reveal the fundamental HE mechanisms. Moreover, the testing on pre-charged sample cannot precisely bridge the H content and mechanical property degradation, due to the uncountable H loss within the dwell time between charging and testing. Therefore, new approaches integrating *in situ* H charging and small-scale mechanical testing are needed to better clarify the interaction between H and individual constituents in materials.

4.1 Small-scale *in situ* Tensile Tests in SEM

The small-scale tensile tests inside SEM provide the opportunity to capture the microstructure and damage evolution through SEM-based techniques such as secondary electron imaging, back-scattered electron imaging, electron backscattered diffraction (EBSD) and electron channeling contrast imaging (ECCI) [69–72]. The tests can be performed for both pre-charged specimens [73–75] and specimens under an *in situ* charging condition. For the former case, it is difficult to precisely quantify the amount of H during the testing and imaging due to the continuous H outgassing. Also, it would be challenging to differentiate whether the possibly probed defect evolution is due to the presence of H or to the H desorption process. The latter was also reported to affect the activity of dislocations [76]. Recently, some novel setups combining *in situ* H charging (performed using H plasma [77] or electrochemically [78]) and SEM observation have been developed, which opens new possibilities of studying the H effect in a more comprehensive manner. For example, Depover and Wan et al. [74, 79] have shown that the H plasma charging provides the possibility to *in situ* charge ferritic or dual-phase materials without causing significant damages on the sample surface. By solely comparing the fatigue crack growth path in a same grain under H-free and

H plasma conditions, a noticeably higher crack growth rate with a reduced plastic zone in the H-containing environment was documented, which was concluded as the result of the restricted dislocation activities due to the ingress of H [79]. In comparison with the conventional pressurized H gas or electrochemical charging methods, a relatively weak embrittlement effect is normally induced by H plasma charging. The effect is more visible at high tensile deformation levels [74] or under cyclic loading conditions where the H effects can be accumulated [79].

4.2 Nanoindentation Testing with *in situ* H Charging

Nanoindentation testing is a method that was originally designed as a hardness measurement tool focusing on small volumes and films [80]. The modern instrumented nanoindentation is capable of testing various mechanical properties such as elastic modulus, fatigue, creep and scratch resistance [81, 82]. During nanoindentation tests, a load–displacement curve (Fig. 4) in the order of μN – nm is continuously recorded with a high resolution, providing the possibility to detect the interaction between dislocations and H on a nano- or microscale. The effect of H on advanced high-strength alloys has been studied by performing nanoindentation tests on pre-charged samples [83, 84]. An enhanced hardness was observed due to the solid solution strengthening by dissolved H [84]. However, a surface hydrogen depletion zone will be formed on pre-charged samples during the nanoindentation test, owing to the outgassing diffusion process. This result indicates that the effect primarily originates from the trapped H instead of diffusible H, since the penetration depth is typically in the range of nanometers for a nanoindentation test. Recently, the *in situ* electrochemical nanoindentation combined with scanning probe microscopy (ECNI-SPM)

has been developed (Fig. 5) [65]. This technique integrates nanoindentation tests with *in situ* H charging to keep a stable and constant surface H concentration. It has shown its advantage in probing the H effect on both the mechanical properties and the discrete events. For the effect of H on mechanical properties, a H-enhanced hardness was detected on several high-strength alloys due to the enhanced retarding stress on dislocation motion and the increased lattice friction between H and dislocations [85–87]. The effect of H on elastic behavior can also be simultaneously determined by ECNI technique. For the discrete events, a H-reduced pop-in load was generally reported on many high-strength alloys, which was proposed as the result of the H-enhanced homogenous dislocation nucleation caused by a reduced

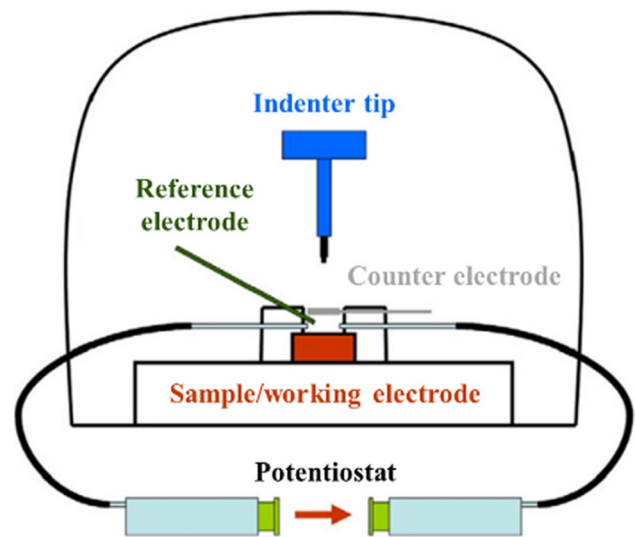


Fig. 5 Schematic drawing of the electrochemical nanoindentation (ECNI) setup. (Reprinted with permission from Ref. [65])

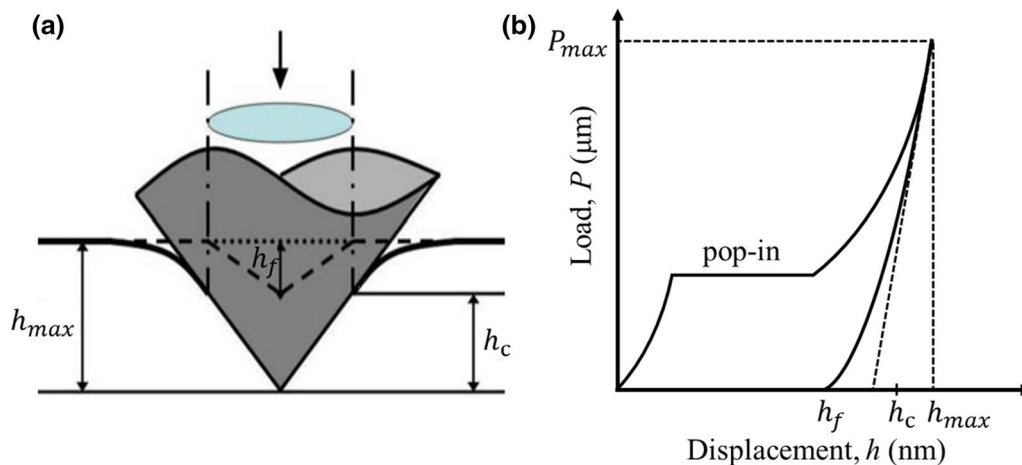


Fig. 4 Schematic drawing of **a** an indentation test at maximum load, **b** the corresponding load–displacement curve

dislocation nucleation energy [64, 65]. Interestingly, it has been detected using ECNI-SPM that only by H charging, it is able to induce surface deformation and phase transformation due to the H-enhanced internal stress [88–91]. These H-charging-induced surface phenomena thus need to be considered in future studies pertaining to the explanation of HE.

4.3 Microcantilever Bending and Pillar Compression Testing Under H Atmosphere

Using the similar nanoindentation-based setup, the microcantilever bending and pillar compression test can also be performed with *in situ* H charging (Figs. 6 and 7). These tests can be carried out in environmental SEM (ESEM) for certain alloys, such as Fe–Al intermetallics where the atomic H was continuously produced by the reaction of aluminum with water vapor used as the environmental condition in ESEM [92]. These microscale tests can also be performed in the same electrochemical charging cell as used for ECNI test or in the atmosphere of H plasma. Moreover, through adding a pre-notch on certain lattice planes of the microcantilevers or milling bi-crystalline micropillars with different types of grain boundaries, a more detailed view of H-assisted cracking along either lattice planes or interfaces can be obtained. These microscale testing approaches allow to eliminate the proximity effect from free surface that is always criticized in *in situ* TEM tests.

The above *in situ* techniques have been carried out on several alloys, such as nickel-based alloy 725, Fe–Al and cantor high-entropy alloys [6, 93]. The results of *in situ* microcantilever tests on an interstitial CoCrFeMnNi high-entropy alloy (Fig. 6) showed clearly different cracking behaviors in H-free (air) and H-charged conditions [93]. In the H-free condition (Fig. 6a, a₁), notch blunting accompanied by abundant slip lines (marked by black lines) indicated a ductile fracture mode with a large amount of plasticity during deformation. In contrast, in the H-charged condition (Fig. 6b, b₁), a sharp cracking and a reduced number of slip lines were observed, elucidating a confined plasticity along the cracking path. Such different cracking behaviors in H-free and H-charged conditions were proposed to be due to the synergistic effect of H-enhanced dislocation nucleation and H-reduced dislocation mobility [6, 93]. Figure 7 shows an example of the *in situ* bi-crystalline micropillar compression test performed on a solution-treated nickel-based Alloy 725 [3]. A H-induced hardening effect was observed from the stress/strain curves, which was attributed to H-enhanced dislocation multiplication and interactions as well as the H-enhanced lattice friction [3]. By adopting transmission-EBSD technique, dislocation behavior along grain boundaries was captured. Transmission-EBSD results on low-angle grain boundary (LAGB) showed a full transmission of dislocations across the grain boundary and relatively homogeneous plastic deformation along micropillars in the H-free condition (Fig. 7a). However, an evident dislocation pileup

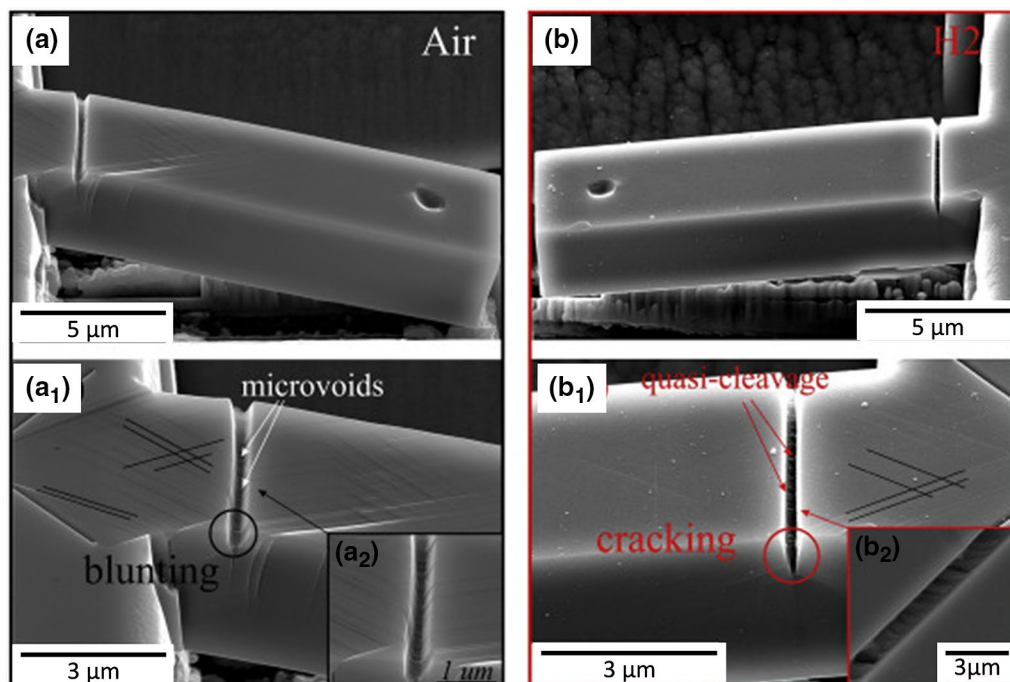


Fig. 6 SEM micrographs showing the deformation behavior of microcantilevers bent in **a–a₁** air, in **b–b₁** H atmosphere. (Reprinted with permission from Ref. [93])

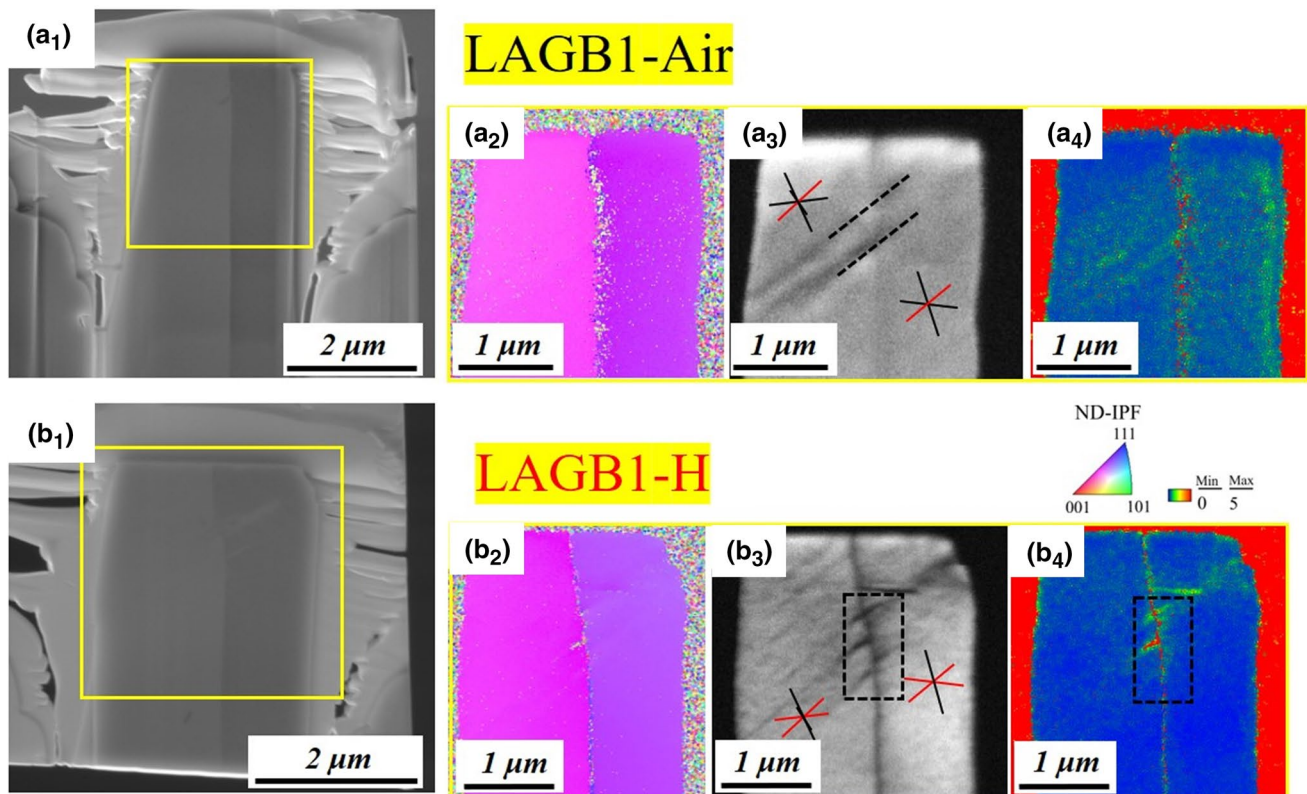


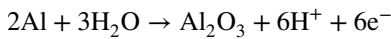
Fig. 7 Micrographs of micropillar lamellae containing a representative low-angle grain boundary (LAGB1) after the compression tests for samples under the **a₁** H-free (air), **b₁** H-charged conditions. Transmission-EBSD results showing the corresponding **a₂**, **b₂** inverse pole figures, **a₃**, **b₃** image quality maps and **a₄**, **b₄** kernel average misorientation (KAM) maps. (Reprinted with permission from Ref. [3])

was observed in the H-charged condition (Fig. 7b), indicating a suppression effect of H to dislocation transmission at specific grain boundaries. These results provide valuable insights on the mechanisms of H-induced cracking behavior.

4.4 New Approaches for Charging Hydrogen

For the above-mentioned small-scale testing approaches, the choice of H-charging method is critical in order to achieve a stable *in situ* H atmosphere without disturbing the mechanical testing process. Up to now, several “direct” and “indirect” H-charging methods have been proposed and are worthwhile to overview. For the “direct” charging method, a glycerol-based solution consisting of borax or phosphorous acid has been widely used for *in situ* nanoindentation, microcantilever bending and micropillar compression tests [64, 94]. This electrolyte is appropriate for preserving the sample surface from corrosion throughout the whole testing procedure due to its extremely low solubility and diffusivity of oxygen. It can also provide a high pressure-like surface H due to its high viscosity at room temperature [73]. However, this electrolyte can only be used in ambient atmosphere (normal pressure). For the tests combining with SEM setup, the

H plasma charging has been used to provide a mild H source under low vacuum condition [79, 95]. One drawback of such charging method is that the amount of plasma-charged H cannot be easily controlled due to the complexity of plasma medium compared with electrochemical charging, where the H can be readily controlled by changing the potential or current. Recently, a new *in situ* H-charging setup was developed, which isolated electrolyte to the backside of sample by a double-wall structured chamber [78]. This setup enables *in situ* H charging under vacuum condition, such as SEM-based techniques. When H diffuses to the sample surface, simultaneous microstructural observation and micromechanical testing can be achieved. As a result, the H-induced microstructural changes can be continuously traced without electrolyte contamination on surface. It needs to mention that this backside charging method is more suitable to metallic materials with BCC lattice structure, which has a much faster H diffusivity than that for FCC structure or BCC–FCC dual-phase structure [13]. The “indirect” charging method can be applied on specific metallic materials that can produce H directly from moisture, such as Fe–Al intermetallics, where atomic H can be produced by the reaction between aluminum and water vapor:



Therefore, given water vapor as the default environment, H-induced cracking can be directly captured using small-scale testing with *in situ* SEM observation [96].

5 Hydrogen Embrittlement in Advanced High-Strength Steels—A Critical Perspective

The study of HE in AHSS has mainly concentrated on the first and second generations (e.g., high-strength ferritic or martensitic [97], DP [98], transformation-induced plasticity (TRIP) [12] and twinning-induced plasticity (TWIP) [7] steels). Among these studies, most investigated the influence of H-charging condition, H content, mechanical and microstructural conditions on the HE susceptibility and H-induced damage characteristics. The active HE mechanisms in these materials, however, are generally less clear. This is partly due to the strong controversies existed among different fundamental HE models, as described in Sect. 2. Further, the extremely fine volume in which H interacts with defects and leads to damages often requires a more careful and higher-resolution characterization beyond SEM-based techniques, which greatly enhances experimental difficulties. On the other hand, the great complexity in AHSS in terms of microstructure and deformation micromechanisms also brings new challenges for understanding HE mechanisms.

In this section, we first overview two HE investigations carried out on two representative AHSS classes (DP [11] and medium-Mn [13] steels) as examples to highlight the complex HE problems and the investigation challenges. Then, we summarize the complexity, critical problems and major challenges of understanding HE mechanisms in AHSS and discuss the future research steps/directions toward this goal.

5.1 Example 1: Hydrogen Embrittlement in Ferrite–Martensite Dual-Phase Steels

Ferrite–martensite DP steels are one of the most widely used AHSS in weight-reduced automotive components. The physical metallurgy behind this material class, i.e., the mixture of both strong and ductile phases to achieve a micromechanical composite effect enabling better strength–ductility synergy, represents an important design strategy for AHSS. The high-strength level and the presence of martensite make such steels generally prone to HE. Here, we overview the related study from Koyama et al. [11], who developed a detailed discussion on the HE mechanisms in such steels based on careful SEM-based postmortem analysis. In their study, one grade of DP steel with a martensite fraction of 55 vol.% (Fig. 8a) was selected. H pre-charging was performed electrochemically for 1 h, which was deemed to be sufficient to make the sample saturated with H based on the evaluation using the effective diffusion coefficient of H in fresh martensite. It was found that H affected both damage nucleation and growth. These two regimes were controlled

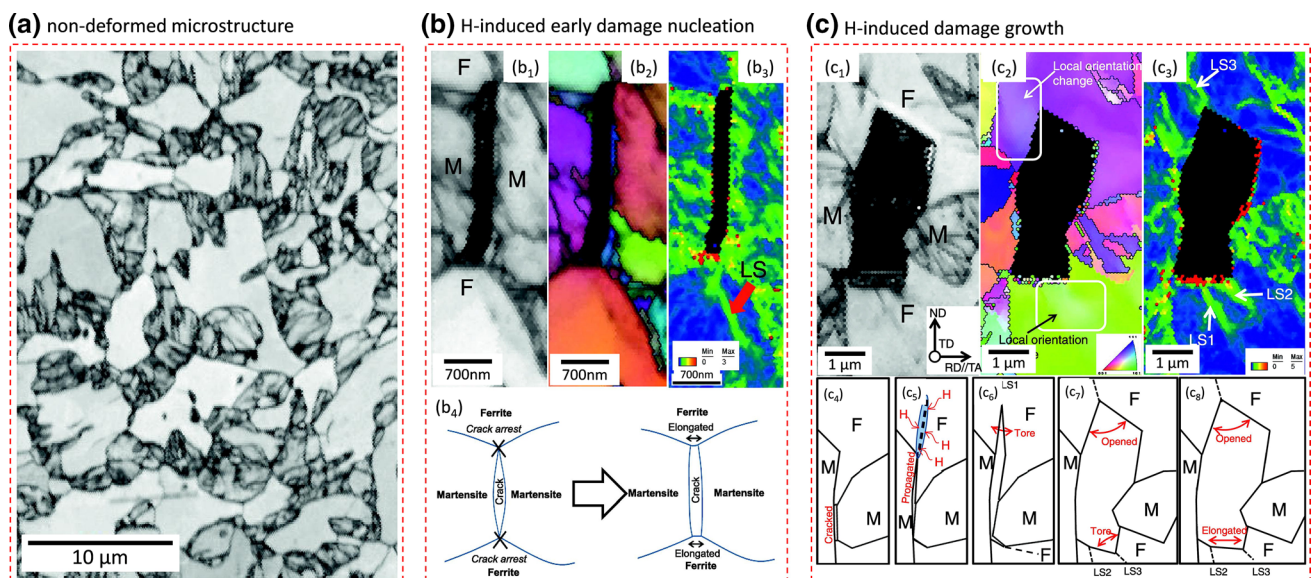


Fig. 8 **a** EBSD image quality (IQ) map showing the initial non-deformed microstructure of the DP steel used in Ref. [11]; **b** EBSD IQ, inverse pole figure (IPF) and kernel average misorientation (KAM) map **b**₁–**b**₃ and schematic diagrams **b**₄ showing the H-induced crack nucleation at prior-austenite grain boundaries, which was proposed to be due to the HEDE effect **c** EBSD results **c**₁–**c**₃ and schematic diagrams **c**₄–**c**₈ showing the H-induced crack propagation inside ferrite close to the crack tip. (Reconstructed with permission from Ref. [11])

by different phases with distinctly different HE mechanisms. For the crack nucleation regime, H promoted the decohesion of prior-austenite grain boundaries (Fig. 8b₁–b₃), which was attributed to the HEDE effect. However, the surrounding ferrite tended to blunt crack propagation by plastic deformation at the nucleated crack tips (Fig. 8b₄). In this case, H could concentrate on the highly strained zones and provide a HELP effect which efficiently promoted crack propagation inside ferrite (as shown from the EBSD results in Fig. 8c₁–c₃ and schematic diagrams in Fig. 8c₄–c₈). The operation of different HE mechanisms in different phases is likely due to their intrinsically different properties and different interactions with H. The very different C content and substructure between ferrite and α' -martensite could significantly influence the strength level, thus the crack driving force, the H trapping [99, 100] and subsequent migration upon deformation, and the resulting localized decohesion and plasticity effects [100].

5.2 Example 2: Hydrogen Embrittlement in Ferrite–austenite TRIP-Aided Medium-Mn Steels

Unlike DP steels with a body-centered cubic (bcc) and body-centered tetragonal (bct) structure where H diffusion is relatively fast (diffusion coefficient above 10^{-12} m²/s at room temperature [101]), and thus, H saturation within the microstructure can be readily achieved, steels with certain fraction of austenite are difficult to be saturated with H. Based on the reported H diffusion coefficient ($D = 10^{-15}$ – 10^{-13} m²/s [102]) in duplex stainless steels with around 40–50% austenite, the diffusion distance ($\sim (Dt)^{0.5}$) of H at room temperature after 10 days

is only about 30–300 μm . The strong contrast between austenite and ferritic phases in terms of H diffusivity and solubility is likely to result in a heterogeneous H distribution. An extreme case occurs when the austenite fraction is relatively low and the H diffusion is governed by percolating ferrite. In this case, the amount of H trapped inside austenite could be limited given a limited charging time. Such heterogeneous H distribution resulting from a heterogeneous microstructure can significantly affect the active HE mechanisms. In the recent work of Sun et al. [13], two types of ferrite–austenite medium-Mn steels were studied using TDS and careful postmortem damage analysis. One steel had a ferrite matrix (~ 75 vol.% α) with austenite islands embedded (Fig. 9a), and the other had an austenite matrix (Fig. 9b). Both steel samples were electrochemically charged for 24 h. The fully connected three-dimensional ferritic network in the first sample was deemed to provide a fast path for H transport, and the austenite islands can be circumvented by H. This suggested that H was mainly trapped at dislocations and grain boundaries inside ferrite, which was supported by the appearance of only one TDS peak and the associated relatively low H desorption activation energy ($E_A = 20$ kJ/mol, Fig. 9a). The segregated H at dislocations provided a HELP effect, which increased the strain incompatibility between ferrite and neighboring phases, thus promoting void nucleation [13]. The dominance of the HELP mechanism in this sample was supported by a dramatically increased (up to ~ 13 times) void nucleation rate by H, the fracture surface and damage analysis, and the insensitivity of HE resistance to applied strain rates [13]. In contrast to the sample with an austenite

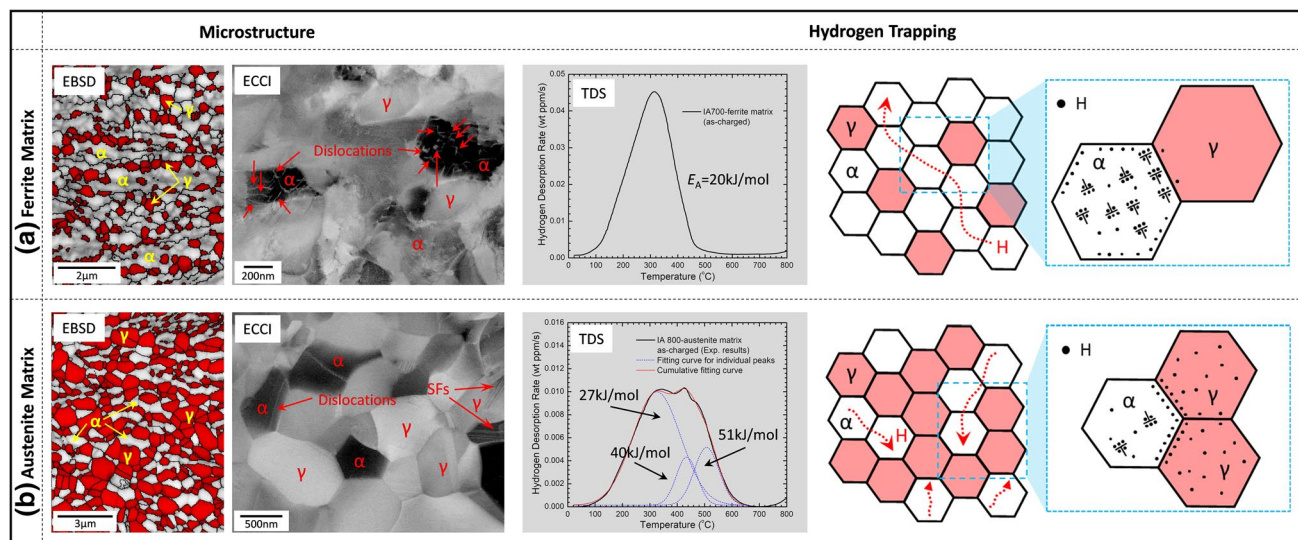


Fig. 9 EBSD and ECCI results, TDS spectrum and schematic diagrams showing the H trapping behavior in a medium-Mn steel with **a** a ferrite matrix, **b** an austenite matrix. (Reconstructed with permission from [13])

matrix, the percolating austenite phase interrupted the efficient diffusion path in ferrite as such H inevitably diffused through the interphase boundaries and austenite and got trapped there. This trapping behavior was supported by the existence of three major peaks in the TDS spectrum and the higher H desorption activation energy for the two higher-temperature peaks ($E_A = 40$ kJ/mol and 51 kJ/mol, Fig. 9b). In this case, the HE was mainly governed by the HEDE mechanism. The initially trapped H at the ferrite–austenite interfaces along with phase transformation-induced H migration to such interface and prior-austenite grain boundaries decreased their cohesive strength and promoted intergranular cracking [13]. This study again demonstrates that different phases and microstructure constituents in AHSS react differently with H, thus showing different embrittlement mechanisms. More importantly, it shows that the initial H distribution and its subsequent migration can greatly affect which phase and the associated HE mechanism are dominant during the failure process.

5.3 Challenges of Revealing Hydrogen Embrittlement in AHSS

The above overviewed two studies have shown great complexities of the HE problem in AHSS, especially pertaining to the activation and prevalence of fundamental mechanisms. It is important to mention that despite systematic and careful experiments conducted in these two studies, the proposed HE mechanisms are only supported by indirect evidence without quantitative and precise direct proof. Significant research efforts thus need to be spent in the future in order to fully understand HE in such complex materials. From the authors' point of view, three major challenges exist in this field, which are described in Fig. 10 and listed as follows.

1. H distribution, trapping and migration upon loading
It is well established that the small H atoms can interact with almost all defects in metals. Its local distribution, atomic trapping and migration upon loading are thus vital for the activation of specific HE mechanisms,

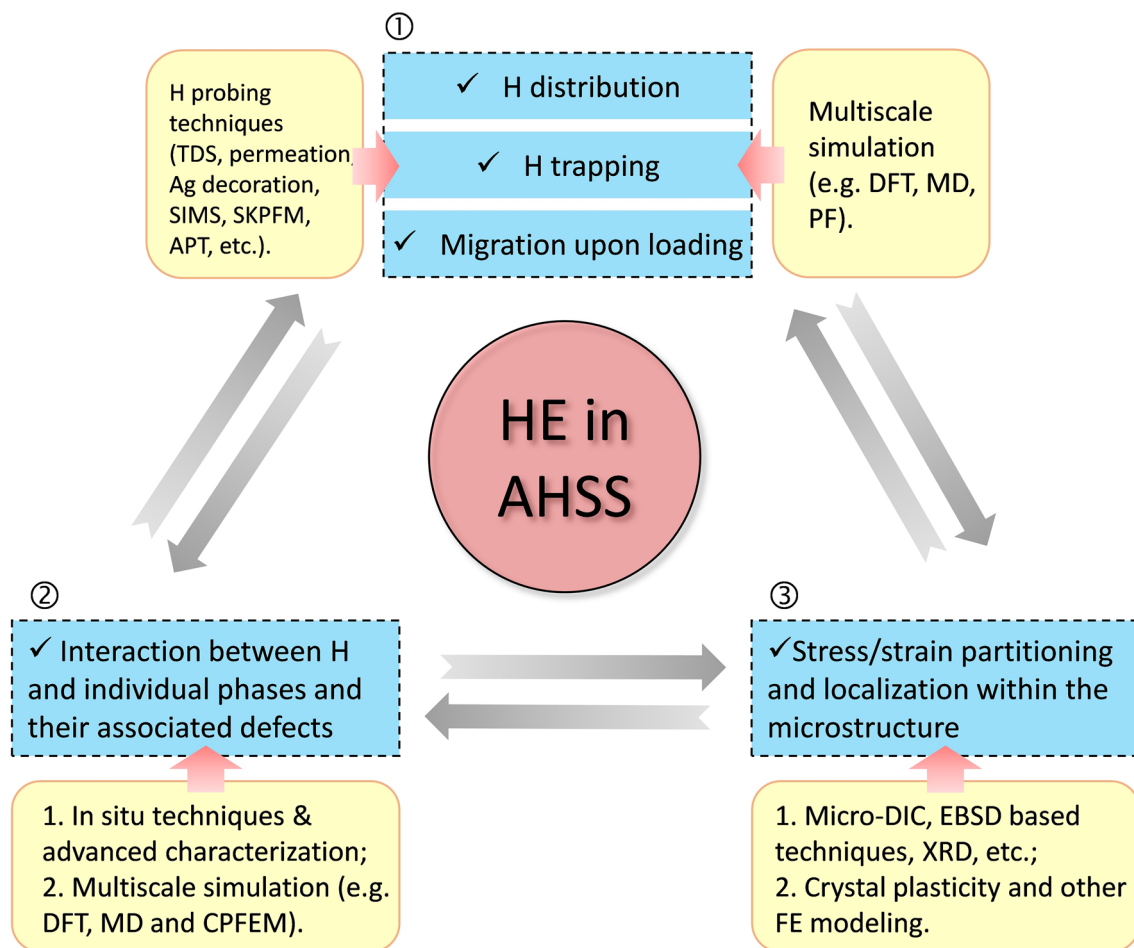


Fig. 10 Schematic diagram showing the major challenges for understanding HE mechanisms in AHSS and common experimental and modeling methods that can be applied to address these challenges

thus the local/global HE resistance. Compared with single-phase model alloys, AHSS have a much more complex microstructure both in non-deformed and deformed states, containing normally multiphases and multiple types of lattice defects [24, 103]. Further, the deformation-driven evolution of microstructure, local stress states and defects is also rather complex and has a significant impact on the local thermodynamics and kinetics of H migration and redistribution. For example, the austenite-to-martensite (α' type) transformation essentially makes the H atoms transfer from an initial low-mobility solute state to a supersaturated and highly mobile state [104–106]. Therefore, without a proper understanding of H trapping and its migration upon loading, any proposed HE mechanisms would seem speculative. This information is especially important when H is not saturated within the whole sample (as shown in Example 2 in Sect. 4.2), which is often the case for the H-induced failure in real applications. Therefore, H probing to acquire the microstructure-specific H distribution and its evolution upon loading would be considered as the first critical step to understand HE in AHSS (Fig. 10). Current experimental techniques for probing H include TDS, silver decoration, scanning Kelvin probe force microscopy (SKPFM), secondary ion mass spectroscopy (SIMS), atom probe tomography (APT), neutron radiography, etc. More details regarding these techniques have been overviewed in Ref. [107]. These experimental methods, however, suffer either the lack of spatial resolution (e.g., TDS), or the lack of temporal resolution (e.g., TDS and APT), or incapability of quantification (e.g., Ag decoration and SKPFM), or significant experimental difficulty (e.g., APT). Therefore, significant research efforts are still in high demand to further advance H probing techniques. Various modeling methods such as DFT, molecular dynamics (MD) and phase-field (PF) methods also need to be combined in order to provide more theoretical foundations regarding H behavior in such materials.

2. Interaction between H and individual phases and their associated defects

Different phases in AHSS normally have a large difference in terms of mechanical property, defects evolution upon loading and H solubility and diffusivity. Such intrinsic difference triggers a different H interaction with individual phases and thus different HE mechanisms, as shown in Example 1 described in Sect. 4.1. Therefore, the H effects on different phases need to be separately treated and investigated. Their respective contribution to the macroscopic H-induced failure also requires a critical assessment. Moreover, the presence of multiple phases essentially produces different types of interphase boundaries [108, 109]. These hetero-interfaces differ

from grain boundaries in terms of the interfacial energy as well as the stress/strain field around the interface [109]. Their interaction with H has not been deeply studied from both experimental and modeling perspectives. The aforementioned micromechanical testing methods in combination with *in situ* H-charging and multiscale simulations (e.g., DFT, MD, PF and crystal plasticity finite element method (CPFEM)) can provide important insights in this field (Fig. 10).

3. Stress/strain partitioning and localization within the microstructure

A high degree of strain/stress partitioning and localization is developed in many AHSS upon loading, resulting from their heterogeneous microstructure and the high mechanical contrast among different phases [24, 25, 110–112]. Further, such local strain/stress states can also be dynamically changed or even altered with plasticity deformation that triggers different deformation mechanisms and strain hardening in different phases. For example, Latypov et al. [23] have found that the high strain-hardening capability of retained austenite in a TRIP- and TWIP-aided medium-Mn steel led to a shift of strain localization initially in austenite to the ferrite phase at later deformation regime. The local strain/stress states and their evolution upon deformation would essentially alter H trapping and migration as well as the local mechanical driving force for damage formation. Such information is thus important to probe, which can be realized by microscale digital image correlation (micro-DIC) [113, 114], X-ray and neutron diffraction [108, 109, 115] and EBSD-based techniques [22] and supported by various modeling methods (e.g., finite element (FE) methods).

6 Summary

This overview discussed the current challenges and opportunities toward understanding HE mechanisms in AHSS. The realization of this task first relies on the accuracy of fundamental HE models proposed in simple model materials, which are still highly debatable. In addition to this point, three other critical questions need be addressed to achieve a full understanding, namely (a) the H distribution, trapping and migration upon loading, (b) the interaction between H and individual phases and their associated defects and (c) stress/strain partitioning and localization within the microstructure. The significant influence of the first two points on the prevalent HE mechanisms was reflected from the overviewed HE study in DP steels and medium-Mn steels. The current developed micromechanical testing techniques in combination with *in situ* H charging can address some of the above challenges. However, much more research efforts

on both experiments and multiscale modelling still need to be carried out. Despite great challenges for understanding fundamental HE mechanisms in AHSS, the strategies of mitigating HE susceptibility in such materials are relatively straightforward [5]. Since the occurrence of HE critically depends on the amount of H and their diffusion within the microstructure regardless of specific HE mechanisms, preventing H ingress and introducing deep traps to reduce H diffusivity are generally effective. Based on this, many methods such as the application of protective coatings and the introduction of V- or Ti-based carbides have been developed [5, 15]. The other strategy lies in improving the intrinsic toughness of the material, such as by producing low-energy interfaces [116] or introducing tough phases [117]. The high toughness of these interfaces or phases can suppress the propagation of H-induced cracks, thus improving the HE resistance. These two strategies can thus serve as guidelines for designing new H-resistant AHSS.

References

- [1] W.H. Johnson, *Proc. R. Soc. London* **23**, 168 (1875)
- [2] R. P. Gangloff, B. P. Somerday (ed.), *Gaseous Hydrogen Embrittlement of Materials in Energy Technologies: the Problem, Its Characterisation and Effects on Particular Alloy Classes* (Elsevier, 2012).
- [3] X. Lu, D. Wang, *J. Mater. Sci. Technol.* **67**, 243 (2020)
- [4] A. Alvaro, I.T. Jensen, N. Kheradmand, O. Løvvik, V. Olden, *Int. J. Hydrog. Energy* **40**, 16892 (2015)
- [5] H.K.D.H. Bhadeshia, *ISIJ Int.* **56**, 24 (2016)
- [6] Y. Deng, A. Barnoush, *Acta Mater.* **142**, 236 (2018)
- [7] M. Koyama, E. Akiyama, Y.K. Lee, D. Raabe, K. Tsuzaki, *Int. J. Hydrog. Energy* **42**, 12706 (2017)
- [8] M.L. Martin, M. Dadfarnia, A. Nagao, S. Wang, P. Sofronis, *Acta Mater.* **165**, 734 (2018)
- [9] I. Robertson, H. Birnbaum, P. Sofronis, in *Dislocations in Solids*, Vol. 15, ed. by J.P. Hirth, L. Kubin (Elsevier, 2009), p. 249.
- [10] A.J. Breen, L.T. Stephenson, B. Sun, Y. Li, O. Kasian, D. Raabe, M. Herbig, B. Gault, *Acta Mater.* **188**, 108 (2020)
- [11] M. Koyama, C.C. Tazan, E. Akiyama, K. Tsuzaki, D. Raabe, *Acta Mater.* **70**, 174 (2014)
- [12] Q. Liu, Q. Zhou, J. Venezuela, M. Zhang, J. Wang, A. Atrens, *Corros. Rev.* **34**, 127 (2016)
- [13] B. Sun, W. Krieger, M. Rohwerder, D. Ponge, D. Raabe, *Acta Mater.* **183**, 313 (2020)
- [14] J. Han, J.H. Nam, Y.K. Lee, *Acta Mater.* **113**, 1 (2016)
- [15] O. Barrera, D. Bombac, Y. Chen, T. Daff, E. Galindo-Nava, P. Gong, D. Haley, R. Horton, I. Katarov, J. Kermodé, *J. Mater. Sci.* **53**, 6251 (2018)
- [16] S. Lynch, *Corros. Rev.* **30**, 105 (2012)
- [17] C. McMahon Jr., *Eng. Fract. Mech.* **68**, 773 (2001)
- [18] M.B. Djukic, G.M. Bakic, V.S. Zeravic, A. Sedmak, B. Rajicic, *Eng. Fract. Mech.* **216**, 106528 (2019)
- [19] M. Nagumo, K. Takai, *Acta Mater.* **165**, 722 (2018)
- [20] S. Lynch, in *Stress Corrosion Cracking*, ed. by V. S. Raja, T. Shoji (Elsevier, 2011), p. 90.
- [21] R. Kirchheim, *Scr. Mater.* **62**, 67 (2010)
- [22] D. An, H. Zhao, B. Sun, S. Zaefferer, *Scr. Mater.* **186**, 341 (2020)
- [23] M.I. Latypov, S. Shin, B.C. De Cooman, H.S. Kim, *Acta Mater.* **108**, 219 (2016)
- [24] D. Raabe, B. Sun, A.K. Da Silva, B. Gault, H.W. Yen, K. Sedighiani, P.T. Sukumar, I.R. Souza Filho, S. Katnagallu, E. Jäggle, *Metall. Mater. Trans. A* **51**, 5517 (2020)
- [25] B. Sun, F. Fazeli, C. Scott, N. Brodusch, R. Gauvin, S. Yue, *Acta Mater.* **148**, 249 (2018)
- [26] B. Sun, F. Fazeli, C. Scott, S. Yue, *Metall. Mater. Trans. A* **47**, 4869 (2016)
- [27] B. Sun, R. Ding, N. Brodusch, H. Chen, B. Guo, F. Fazeli, D. Ponge, R. Gauvin, S. Yue, *Mater. Sci. Eng. A* **749**, 235 (2019)
- [28] R. Oriani, *Bunsen-Ges. Phys. Chem.* **76**, 848 (1972)
- [29] A.R. Troiano, *Metallogr. Microstruct. Anal.* **5**, 557 (2016)
- [30] T. Perng, C. Altstetter, *Metall. Mater. Trans. A* **18**, 123 (1987)
- [31] W.W. Gerberich, R. Oriani, M.J. Lji, X. Chen, T. Foecke, *Philos. Mag. A* **63**, 363 (1991)
- [32] M. Yamaguchi, J. Kameda, K.I. Ebihara, M. Itakura, H. Kaburaki, *Philos. Mag. A* **92**, 1349 (2012)
- [33] G. A. Young, J. R. Scully, in *International Conference on Hydrogen Effects on Material Behavior and Corrosion Deformation Interactions*, Moran, 2002.
- [34] D. Li, R.P. Gangloff, J.R. Scully, *Metall. Mater. Trans. A* **35**, 849 (2004)
- [35] J. Song, W. Curtin, *Acta Mater.* **59**, 1557 (2011)
- [36] M. Seah, *Acta Metall.* **28**, 955 (1980)
- [37] B. Sun, D. Palanisamy, D. Ponge, B. Gault, F. Fazeli, C. Scott, S. Yue, D. Raabe, *Acta Mater.* **164**, 683 (2019)
- [38] D. Jiang, E.A. Carter, *Acta Mater.* **52**, 4801 (2004)
- [39] R. Matsumoto, S. Taketomi, S. Matsumoto, N. Miyazaki, *Int. J. Hydrog. Energy* **34**, 9576 (2009)
- [40] A. Tahir, R. Janisch, A. Hartmaier, *Mater. Sci. Eng. A* **612**, 462 (2014)
- [41] C.D. Beachem, *Metall. Mater. Trans. B* **3**, 441 (1972)
- [42] H.K. Birnbaum, P. Sofronis, *Mater. Sci. Eng. A* **176**, 191 (1994)
- [43] P. Sofronis, H.K. Birnbaum, *J. Mech. Phys. Solids* **43**, 49 (1995)
- [44] S. Wang, N. Hashimoto, S. Ohnuki, *Sci Rep.* **3**, 2760 (2013)
- [45] M. Itakura, H. Kaburaki, M. Yamaguchi, T. Okita, *Acta Mater.* **61**, 6857 (2013)
- [46] J. Song, W. Curtin, *Acta Mater.* **68**, 61 (2014)
- [47] J. Song, W. Curtin, *Nat. Mater.* **12**, 145 (2013)
- [48] D. Xie, S. Li, M. Li, Z. Wang, P. Gumbsch, J. Sun, E. Ma, J. Li, Z. Shan, *Nat. Commun.* **7**, 13341 (2016)
- [49] P. Ferreira, I. Robertson, H. Birnbaum, *Acta Mater.* **46**, 1749 (1998)
- [50] D. Shih, I. Robertson, H. Birnbaum, *Acta Metall.* **36**, 111 (1988)
- [51] T. Tabata, H. Birnbaum, *Scr. Metall.* **17**, 947 (1983)
- [52] K. Christmann, *Prog. Surf. Sci.* **48**, 15 (1995)
- [53] P. Ferrin, S. Kandoi, A.U. Nilekar, M. Mavrikakis, *Surf. Sci.* **606**, 679 (2012)
- [54] H. Johnson, Hydrogen gas embrittlement, Paper presented at the Conference on Hydrogen in Metals: Effect on Properties, Selection and Design, Seven Springs, Pennsylvania, September 1973.
- [55] M. Nagumo, K. Ohta, H. Saitoh, *Scr. Mater.* **40** (1999).
- [56] M. Nagumo, *Mater. Sci. Technol.* **20**, 940 (2004)
- [57] M. Nagumo, M. Nakamura, K. Takai, *Metall. Mater. Trans. A* **32**, 339 (2001)
- [58] M. Nagumo, K. Takai, *Acta Mater.* **165**, 722 (2019)
- [59] K. Sakaki, T. Kawase, M. Hirato, M. Mizuno, H. Araki, Y. Shirai, M. Nagumo, *Scr. Mater.* **55**, 1031 (2006)
- [60] R. Kirchheim, *Int. J. Mater. Res.* **100**, 483 (2009)
- [61] T. Neeraj, R. Srinivasan, J. Li, *Acta Mater.* **60**, 5160 (2012)
- [62] R. Kirchheim, *Acta Mater.* **55**, 5129 (2007)
- [63] R. Kirchheim, *Acta Mater.* **55**, 5139 (2007)
- [64] D. Wang, X. Lu, Y. Deng, X. Guo, A. Barnoush, *Acta Mater.* **166**, 618 (2019)
- [65] A. Barnoush, H. Vehoff, *Acta Mater.* **58**, 5274 (2010)

- [66] C. Zapffe, C. Sims, *Trans. AIME* **145**, 225 (1941)
- [67] R. Oriani, *Annu. Rev. Mater. Sci.* **8**, 327 (1978)
- [68] Y. Chang, W. Lu, J. Guénolé, L.T. Stephenson, A. Szczepaniak, P. Kontis, A.K. Ackerman, F.F. Dear, I. Mouton, X. Zhong, *Nat. Commun.* **10**, 942 (2019)
- [69] I. Gutierrez-Urrutia, F. Archie, D. Raabe, F.K. Yan, N.R. Tao, K. Lu, *Sci. Technol. Adv. Mater.* **17**, 29 (2016)
- [70] J. Zhang, D. Raabe, C.C. Tasan, *Acta Mater.* **141**, 374 (2017)
- [71] D. Yan, C.C. Tasan, D. Raabe, *Acta Mater.* **96**, 399 (2015)
- [72] J. Nellessen, S. Sandlöbes, D. Raabe, *Acta Mater.* **87**, 86 (2015)
- [73] X. Lu, D. Wang, D. Wan, Z.B. Zhang, N. Kheradmand, A. Barnoush, *Acta Mater.* **179**, 36 (2019)
- [74] T. Depover, D. Wan, D. Wang, A. Barnoush, K. Verbeken, *Mater. Charact.* **167** (2020).
- [75] D. Wang, X. Lu, D. Wan, X. Guo, R. Johnsen, *Mater. Sci. Eng. A* **140638** (2020).
- [76] M. Koyama, S. M. Taheri-Mousavi, H. Yan, J. Kim, B. C. Cameron, S. S. Moeini-Ardakani, J. Li, C. C. Tasan, *Sci. Adv.* **6**, eaaz1187 (2020).
- [77] A. Massone, A. Manhard, W. Jacob, A. Drexler, W. Ecker, A. Hohenwarter, S. Wurster, D. Kiener, *Rev. Sci. Instrum.* **91**, 043705 (2020)
- [78] J. Kim, C.C. Tasan, *Int. J. Hydrog. Energy* **44**, 6333 (2019)
- [79] D. Wan, Y. Deng, J.I.H. Meling, A. Alvaro, A. Barnoush, *Acta Mater.* **170**, 87 (2019)
- [80] N.G. Chechenin, J. Böttiger, J.P. Krog, *Thin Solid Films* **261**, 228 (1995)
- [81] D. Beegan, S. Chowdhury, M.T. Laugier, *Surf. Coat. Technol.* **201**, 5804 (2007)
- [82] W.C. Oliver, G.M. Pharr, *J. Mater. Res.* **19**, 3 (2004)
- [83] D.K. Han, Y.M. Kim, H.N. Han, H.K.D.H. Bhadeshia, D.W. Suh, *Scr. Mater.* **80**, 9 (2014)
- [84] Y. Zhao, D.H. Lee, J.A. Lee, W.J. Kim, H.N. Han, U. Ramamurthy, J.Y. Suh, J.I. Jang, *Int. J. Hydrog. Energy* **42**, 12015 (2017)
- [85] T. Depover, T. Hajilou, D. Wan, D. Wang, A. Barnoush, K. Verbeken, *Mater. Sci. Eng. A* **754**, 613 (2019)
- [86] A.S. Ebner, S. Brinckmann, E. Plesiutchnig, H. Clemens, R. Pippan, V. Maier-Kiener, *JOM* **72**, 5 (2020)
- [87] N. Kheradmand, R. Johnsen, J.S. Olsen, A. Barnoush, *Int. J. Hydrog. Energy* **41**, 704 (2016)
- [88] M. Asgari, R. Johnsen, A. Barnoush, *Int. J. Hydrog. Energy* **38**, 15520 (2013)
- [89] X. Lu, Y. Ma, M. Zamanzade, Y. Deng, D. Wang, W. Bleck, W.W. Song, A. Barnoush, *Int. J. Hydrog. Energy* **44**, 20545 (2019)
- [90] D. Wang, X. Lu, D. Wan, Z. Li, A. Barnoush, *Scr. Mater.* **173**, 56 (2019)
- [91] D. Wang, X. Lu, Y. Deng, D. Wan, Z. Li, A. Barnoush, *Intermetallics* **114**, 106605 (2019)
- [92] Y. Deng, T. Hajilou, D. Wan, N. Kheradmand, A. Barnoush, *Scr. Mater.* **127**, 19 (2017)
- [93] X. Lu, D. Wang, Z. Li, Y. Deng, A. Barnoush, *Mater. Sci. Eng. A* **762**, 138114 (2019)
- [94] X. Lu, Y. Ma, D. Wang, *Mater. Sci. Eng. A* **792**, 139785 (2020)
- [95] D. Wan, Y. Deng, A. Barnoush, *Scr. Mater.* **151**, 24 (2018)
- [96] B.R.S. Rogne, N. Kheradmand, Y. Deng, A. Barnoush, *Acta Mater.* **144**, 257 (2018)
- [97] J. Venezuela, Q. Liu, M. Zhang, Q. Zhou, A. Atrens, *Corros. Rev.* **34**, 153 (2016)
- [98] C.C. Tasan, M. Diehl, D. Yan, M. Bechtold, F. Roters, L. Schemmann, C. Zheng, N. Peranio, D. Ponge, M. Koyama, *Ann. Rev. Mater. Res.* **45**, 391 (2015)
- [99] A. Turk, G.R. Joshi, M. Gintalas, M. Callisti, P.E. Rivera-Díaz-del-Castillo, E.I. Galindo-Nava, *Acta Mater.* **194**, 118 (2020)
- [100] W. Geng, V. Wang, J.X. Li, N. Ishikawa, H. Kimizuka, K. Tsuzaki, S. Ogata, *Scr. Mater.* **149**, 79 (2018)
- [101] J. Sun, T. Jiang, Y. Sun, Y. Wang, Y. Liu, *J. Alloy. Compd.* **698**, 390 (2017)
- [102] V. Olden, A. Saai, L. Jemblie, R. Johnsen, *Int. J. Hydrog. Energy* **39**, 1156 (2014)
- [103] B. Sun, N. Vanderesse, F. Fazeli, C. Scott, J. Chen, P. Bocher, M. Jahazi, S. Yue, *Scr. Mater.* **133**, 9 (2017)
- [104] M. Koyama, Y. Abe, K. Saito, E. Akiyama, K. Takai, K. Tsuzaki, *Scr. Mater.* **122**, 50 (2016)
- [105] T. Hojo, M. Koyama, N. Terao, K. Tsuzaki, E. Akiyama, *Int. J. Hydrog. Energy* **44**, 30472 (2019)
- [106] J.H. Ryu, Y.S. Chun, C.S. Lee, H. Bhadeshia, D.W. Suh, *Acta Mater.* **60**, 4085 (2012)
- [107] M. Koyama, M. Rohwerder, C.C. Tasan, A. Bashir, E. Akiyama, K. Takai, D. Raabe, K. Tsuzaki, *Mater. Sci. Technol.* **33**, 1481 (2017)
- [108] B. Sun, Y. Ma, N. Vanderesse, R.S. Varanasi, W. Song, P. Bocher, D. Ponge, D. Raabe, *Acta Mater.* **178**, 10 (2019)
- [109] Y. Ma, B. Sun, A. Schökel, W. Song, D. Ponge, D. Raabe, W. Bleck, *Acta Mater.* **200**, 389 (2020)
- [110] B. Sun, F. Fazeli, C. Scott, X. Yan, Z. Liu, X. Qin, S. Yue, *Scr. Mater.* **130**, 49 (2017)
- [111] B. Sun, H. Aydin, F. Fazeli, S. Yue, *Metall. Mater. Trans. A* **47**, 1782 (2016)
- [112] B. Sun, F. Fazeli, C. Scott, B. Guo, C. Aranas Jr., X. Chu, M. Jahazi, S. Yue, *Mater. Sci. Eng. A* **729**, 496 (2018)
- [113] A. Dutta, D. Ponge, S. Sandlöbes, D. Raabe, *Materialia* **5**, 100252 (2019)
- [114] Z. Zhang, Z. Yang, S. Lu, A. Harte, R. Morana, M. Preuss, *Nat. Commun.* **11**, 4890 (2020)
- [115] P.J. Gibbs, B. De Cooman, D.W. Brown, B. Clausen, J.G. Schroth, M.J. Merwin, D.K. Matlock, *Mater. Sci. Eng. A* **609**, 323 (2014)
- [116] S. Bechtle, M. Kumar, B.P. Somerday, M.E. Launey, R.O. Ritchie, *Acta Mater.* **57**, 4148 (2009)
- [117] M. Wang, C.C. Tasan, M. Koyama, D. Ponge, D. Raabe, *Metall. Mater. Trans. A* **46**, 3797 (2015)



Binhan Sun received his Bachelor (2011) and Master (2013) degree at School of Materials and Metallurgy, Northeastern University, China. He then joined McGill University, Canada where he obtained his Ph.D. in 2017. In 2018, he received the Humboldt Research Fellowship and went to Max-Planck-Institut für Eisenforschung (MPIE) as a Postdoctoral Researcher. He is now the Topical Leader of Hydrogen Embrittlement in High-Performance Alloys in MPIE. His main research focus is processing-

microstructure-mechanical property correlations of advanced steels, with particular interest in fundamental phase transformation, deformation and damage mechanisms, and hydrogen embrittlement. He has now published near 40 peer-reviewed papers in well-reputed journals such as *Acta Mater.*, *Scripta Mater.* and *Science Advances*. He has attended more than 10 international conferences. In the meantime, he also serves as independent reviewer for more than 20 journals and a guest editor for three SCI journals.